Measurement of the gravitational constant G in space (SEE Project): sensitivity to orbital parameters and space charge effect

A. D. Alexeev, K. A. Bronnikov, N. I. Kolosnitsyn, M. Yu. Konstantinov, V. N. Melnikov and A. J. Sanders

Abstract. We describe some new estimates concerning the recently proposed SEE (Satellite Energy Exchange) experiment for measuring the gravitational interaction parameters in space. The experiment entails precision tracking of the relative motion of two test bodies (a heavy ''Shepherd'', and a light ''Particle'') on board a drag-free space capsule. The new estimates include (i) the sensitivity of Particle trajectories and G measurement to the Shepherd quadrupole moment uncertainties; (ii) the measurement errors of G and the strength of a putative Yukawa-type force whose range parameter λ may be either of the order of a few metres or close to the Earth radius; (iii) a possible effect of the Van Allen radiation belts on the SEE experiment due to test-body electric charging. The main conclusions are that (i) the SEE concept may allow G to be measured with an uncertainty of less than 1 part in 10^7 and progress up to two orders of magnitude is possible in the assessment of possible Yukawa forces and (ii) Van Allen charging of test bodies is a significant problem but it may be solved by existing methods.

1. Introduction

The SEE concept of a space-based gravitational experiment was suggested in the early 1990s [1] and was aimed at precisely measuring the gravitational interaction parameters: the gravitational constant G, possible violations of the equivalence principle measured by the Eötvös parameter η, time variations of G, and hypothetical non-Newtonian gravitational forces (parametrized by the Yukawa strength α and range λ). Such tests are intended to overcome the limitations of the current methods of ground-based experimentation and observation of astronomical phenomena and to fill gaps left by them. The significance of new measurements is clear, as nearly all modified theories of gravity and unified theories predict some violations of the equivalence principle (EP), either by deviations from the Newtonian law (inverse-square law, ISL) or by composition-dependent (CD) gravity accelerations, due to the appearance of new possible massive particles (partners); time variations of G ($\dot{G}$) are also generally predicted [2, 3].

As gravitational forces are so very small, precision-measurement techniques have been at the core of terrestrial gravity research for two centuries. However, increasing evidence is accumulating which indicates that terrestrial methods have plateaued in accuracy and are unlikely to achieve significant accuracy gains in the future. Ref. [4] describes the contemporary situation relative to the measurements of G and $\dot{G}$.

There is considerable evidence that the uncertainty in G has plateaued at about 100 ppm (1 part in 10^4) [5-8]. Most of the stated uncertainties in recent experiments are of the order of 100 ppm. Moreover, the scatter (1 σ) about the mean is about 140 ppm. An exception is the recent paper by Gundlach and Merkowitz [9], which reports an uncertainty of about 14 ppm in G measurement using a dynamically driven torsion balance. Their reported value of G agrees with the previous measurements within their uncertainties. This work is unique for the moment and needs confirmation by other experimental groups using alternative methods.

A. D. Alexeev,[1] K. A. Bronnikov,[2] N. I. Kolosnitsyn,[3] M. Yu. Konstantinov[4] and V. N. Melnikov:[5] RGS, 3-1 M. Ulyanovoy St., Moscow 117313, Russian Federation.
1. e-mail: ada@mics.msu.su
2. e-mail: kb@rgs.mccme.ru
3. e-mail: nikkols@orc.ru
4. e-mail: konst@rgs.phys.msu.su
5. e-mail: melnikov@rgs.phys.msu.su Temporary address: CINVESTAV, Apartado Postal 14-740, Mexico 07360, D.F. Mexico; e-mail: melnikov@fis.cinvestav.mx
A.J. Sanders:[6] Dept. of Physics and Astronomy, University of Tennessee, Knoxville, TN 37996-1200, USA.
e-mail: asanders@utkux.utcc.utk.edu

It might seem that the problems of terrestrial apparatus must inexorably yield to new technologies – that the promise of ever-increasing sensitivities would also lead to ever-improving accuracy. However, this may not be true, as it is the intrinsically weak nature of the force and the resulting systematic errors which arise in its isolation and measurement that limit the ultimate attainable accuracy in terrestrial experiments [4].

The EP may be tested by searching for either violations of the ISL or CD effects in gravitational free fall.

In the watershed year of 1986, Fischbach et al. startled the physics community by showing that Eötvös's famous turn-of-the-century experiment is much less decisive as a null result than was generally believed [10, 11]. Prior to this time, experiments by Dicke [12] and Braginsky [13] had demonstrated the universality of free fall (UFF) to very high accuracy with respect to several metals falling in the gravitational field of the Sun (the Eötvös parameter η was ultimately found to be smaller than 10^{-12}). The interpretation of these results at the time was that they validated the UFF.

Since 1986 it has become customary to parametrize possible apparent EP violations as if due to a Yukawa particle with a Compton wavelength λ. This approach unites both ISL and CD effects very naturally, while the parameter values in the Yukawa potential suggest which experimental conditions are required to detect the new interaction.

Following the conjecture of Fischbach et al., ISL and CD tests were undertaken by many investigators. Although a number of anomalies were initially reported, nearly all of these were eventually explained in terms of overlooked systematic errors or extreme sensitivity to models, while most investigators obtained null results. However, a positive result for a deviation from the Newtonian law (ISL) was obtained (and interpreted in terms of a Yukawa-type potential) in the range of 20 m to 500 m by Achilli and colleagues [14]; this needs to be verified in other independent experiments.

For reviews of terrestrial searches for non-Newtonian gravity, see [15-17].

The idea of the SEE method is to study the relative motion of two bodies on board a drag-free Earth satellite using horseshoe-type trajectories, previously well-known in planetary satellite astronomy: if the lighter body (the "Particle") is moving along a lower orbit than the heavier one (the "Shepherd") and approaching from behind, then the Particle almost overtakes the Shepherd, but it gains energy due to their gravitational interaction, passes therefore to a higher orbit and begins to lag behind. The interaction phase can be studied within a drag-free capsule (a cylinder up to 20 m long, about 1 m in diameter) where the Particle can loiter as long as 10^5 seconds. It was claimed that the SEE method exceeded in accuracy all other suggestions, at least with respect to G and α for λ of the order of metres. Some design features were considered, making it possible to reduce various sources of uncertainty to a negligible level. It was concluded, in particular, that the most favourable orbits are the Sun-synchronous, continuous-sunlight orbits situated at altitudes between 1390 km and 3330 km [1].

Since the origin of the SEE concept, the development has focused on critical analyses of orbital parameters and satellite performance and the assessment of critical hardware requirements. All indications from this work are that the SEE concept is feasible and practicable [18].

At the present stage it can be asserted that, although space is a challenging environment for research, its inherent quietness can be exploited to make very accurate determinations of G and other gravitational parameters, provided that care is taken to understand the many physical phenomena in space which have the potential to vitiate accuracy. A distinctive feature of an SEE mission is its capability to perform such determinations simultaneously on multiple parameters, making it one of the most promising proposals.

To be more specific, let us enumerate the suggested SEE tests and measurements and show their expected uncertainty as currently estimated:

Test/measurement	*Relative standard uncertainty*
EP/ISL at a few metres	2×10^{-7}
EP/CD at a few metres	$< 10^{-7}$ $(\alpha < 10^{-4})$
EP/ISL at $\sim R_\oplus$	$< 10^{-10}$
G	3.3×10^{-7}
$\dot{G}/G$	$< 10^{-13}$ in one year

The last estimate is only tentative; the subject is under study.

This paper describes the principles of the SEE experiment and presents some new evaluations concerning the opportunities offered by the SEE concept and its yet-unresolved difficulties. In Section 2, on the basis of computer simulations of Particle trajectories, we describe some general properties of Particle trajectories in short capsules (Particle-Shepherd separation from 2 m to 5 m), and their sensitivity to the value of the parameters of the gravitational interaction, and we estimate the requirements to the Shepherd quadrupole moment uncertainty. Section 3 shows the results of simulations of the measurement procedure itself, which allows the possible measurement accuracy to be estimated with respect to G and α for λ of the order of either metres or the Earth's radius. Section 4 discusses a spurious effect of test-body electric charging when the satellite orbit passes through the Van Allen radiation belts, rich in high-energy protons. Section 5 is a conclusion.

In what follows, the term "orbit" applies to satellite (or Shepherd) motion around the Earth, while the words "trajectory" or "path" apply to Particle motion with respect to the Shepherd inside the capsule.

2. Simulations of Particle trajectories

In previous studies of the SEE Project it was assumed that the capsule was about 20 m long and the initial Shepherd-Particle separation x_0 along the capsule axis was as great as 18 m; some estimations were also made for 5 m $\leq x_0 \leq$ 10 m. The Shepherd mass was taken to be $M = 500$ kg and the Particle mass $m = 0.1$ kg. The present study retains these values, with the exception of the cases noted below.

In this section we describe some characteristic features of Particle trajectories in short capsules (Particle-Shepherd separation 2 m $\leq x_0 \leq$ 5 m) with the Shepherd mass reduced to $M = 200$ kg. Our goal is to determine the properties of trajectories in the case considered, and the sensitivity of the trajectories to the uncertainty of the orbit radius and the values of the Newtonian gravitational constant and the Shepherd quadrupole moment, J_2. As in our previous studies, the capsule diameter is assumed to be 1 m.

The reason for considering the short capsule, the Shepherd with reduced mass and the quadrupole moment uncertainty is economical and technological in origin, in that it is hard to produce a spherical symmetric Shepherd to the required accuracy. To avoid the inclusion of δJ_2 in the set of parameters to be determined in the experiment, it is useful to know which values of δJ_2 will be negligible, since an increase in the number of parameters leads to serious problems in data processing.

2.1 Equations of motion and initial data

For simplicity, we assume that the relative motion of the test bodies inside the capsule occurs in the satellite orbital plane. This simplification is purely technical because, as found in our previous studies, the three-dimensional nature of the Particle motion does not change the main estimates.

The reduced Lagrangian of the Particle motion in the considered case is

$$L = \frac{M}{2}(\dot{R}^2 + R^2\dot{\varphi}^2) + \frac{m}{2}\left[\dot{r}^2 + r^2(\dot{\varphi}+\dot{\psi})^2\right] + G\frac{M_\oplus m}{r} + G\frac{Mm}{s}\times \left\{1 + J_2\left(\frac{r_\mathrm{s}}{s}\right)^2 P_2(\cos\theta)\right\}\left(1 + \alpha \mathrm{e}^{-s/\lambda}\right), \quad (1)$$

where (R, φ) are the Earth-centred polar coordinates of the Shepherd in the orbital plane; $r = \sqrt{[(R+y)^2 + x^2]}$ and ψ are the Earth-centred polar coordinates of the Particle; x and y are the Shepherd-centred Particle coordinates, where x is the "horizontal" one, i.e. along the orbit and simultaneously along the capsule, and y is the "vertical" one, along the Earth-Shepherd radius vector; $s = \sqrt{(x^2 + y^2)}$ is the Particle-Shepherd separation; $M_\oplus$, M and m are the Earth, Shepherd and Particle masses, respectively; J_2 is the quadrupole moment of the Shepherd, r_s is its radius and P_2 is the Legendre polynomial

$$P_2(\cos\theta) = (3\cos^2\theta - 1)/2,$$

where θ is the angle between the line connecting the centres of the test bodies and the Shepherd equatorial plane. It is easy to see that if the Shepherd symmetry axis is in its orbital plane, then $\theta = \theta_0 = -\arctan(y/x) + \varphi$. If the symmetry axis of the Shepherd is orthogonal to its orbital plane, then $\theta = 0$. In general, if χ is the angle between the Shepherd symmetry axis and its orbital plane, then $\theta = \theta_0 \cos\chi$. Hence the influence of J_2 on the Particle motion is minimum if the Shepherd symmetry axis lies in its orbital plane and is maximum if they are mutually orthogonal.

For simplicity (and taking into account the corresponding estimate) we neglect the influence of the Particle on the Shepherd, so the Shepherd trajectory is considered as given. Then, varying the above Lagrangian with respect to x and y, taking into account that $M \gg m$ and $R \gg s$, we arrive at the following equations of Particle motion with respect to the Shepherd:

$$\frac{\mathrm{d}^2x}{\mathrm{d}t^2} = 2\dot{y}\dot{\varphi} + x\left\{\dot{\varphi}^2 - \frac{GM_\oplus}{r^3}\right\} - \frac{2\dot{R}\dot{\varphi}y}{R} - \frac{G\overline{M}}{s^3}x\left\{1 + J_2\left(\frac{r_\mathrm{s}}{s}\right)^2 P_2(\cos\theta)\right\} - \alpha x\frac{G\overline{M}}{s^2}\left\{1 + J_2\left(\frac{r_\mathrm{s}}{s}\right)^2 P_2(\cos\theta)\right\} \left(\frac{1}{s} + \frac{1}{\lambda}\right)\mathrm{e}^{-s/\lambda} + \frac{G\overline{M}r_0^2}{2s^5}J_2\left(1 + \alpha\,\mathrm{e}^{-s/\lambda}\right)\times [x(1 + 3\cos 2\theta) + 3y\sin 2\theta\cos\chi]; \quad (2)$$

$$\frac{\mathrm{d}^2y}{\mathrm{d}t^2} = -2\dot{x}\dot{\varphi} + (R+y)\left\{\dot{\varphi}^2 - \frac{GM_\oplus}{r^3}\right\} + \frac{2\dot{R}\dot{\varphi}x}{R} - \frac{G\overline{M}}{s^3}y\left\{1 + J_2\left(\frac{r_\mathrm{s}}{s}\right)^2 P_2(\cos\theta)\right\} - \alpha y\frac{G\overline{M}}{s^2}\left(\frac{1}{s} + \frac{1}{\lambda}\right)\left\{1 + J_2\left(\frac{r_\mathrm{s}}{s}\right)^2 P_2(\cos\theta)\right\}\mathrm{e}^{-s/\lambda} + \frac{G\overline{M}r_0^2}{s^5}J_2\left(1 + \alpha\,\mathrm{e}^{-s/\lambda}\right)\times [3x\sin 2\theta\cos\chi + y(1 - 3\cos\theta)]; \quad (3)$$

where $\overline{M} = M + m$.

Two kinds of initial conditions for (2) and (3) were used during the simulations. First, we used the so-called "standard" initial conditions, taking the Particle velocity components $\dot{x}(0)$ and $\dot{y}(0)$ corresponding to its unperturbed (i.e. without the M-m interaction) orbital motion distinguished from the Shepherd's orbit only by its radius (for circular orbits) or semi-major axis (for elliptic orbits). Assuming that the Particle motion

begins right at the moment when the Shepherd passes its perigee, these conditions have the form

$$x(0) = x_0, \qquad y(0) = y_0,$$
$$\dot{x}(0) = \frac{\omega e' y_0}{2(1-e)^2}, \qquad \dot{y}(0) = -\frac{\omega e x_0}{e'(1-e)}, \tag{4}$$

where $\omega^2 = GM_\oplus/R_0^3$, R_0 is the Shepherd orbital radius (at the perigee), e is the orbital eccentricity and $e' = \sqrt{(1-e^2)}$.

For clarity, the relations (4) are written in the linear approximation in the variables x and y. Higher-order approximations were used in the simulation process as well.

The second kind of initial condition corresponds to small variations of initial velocities with respect to their "standard" values.

The set of equations (2, 3) was solved numerically using the software developed previously [18] to analyse the SEE Project. On the basis of these numerical solutions, we considered two types of Particle trajectory, corresponding to different choices of the initial data: (i) approximately U-shaped ones; and (ii) cycloidal ones, containing loops (see more details on the trajectories in [1, 18], for orbital altitudes $H_{\rm orb} = 500$ km, 1500 km and 3000 km.

2.2 General characteristics of trajectories in a short capsule

Reduction of the Shepherd mass leads to a reduction in distance between the libration points L_1 and L_2. As a result, the region where the horseshoe orbits exist is also reduced and the turning points for the horseshoe orbits become closer to the Shepherd. Thus, for a Shepherd mass of $M = 200$ kg, the positions of the turning points of the horseshoe orbits starting, for example, at $x_0 = 18$ m and 0.1 m$\leq |y_0| \leq 0.3$ m are placed in the region $x \leq 5$ m for all orbits whose altitude H lies in the interval 500 km to 3000 km. The use of short trajectories, with $x_0 \leq 5$ m, and especially extremely short trajectories, with $x_0 = 2$ m, leads to additional limitations on the initial conditions.

Numerical simulation shows that to avoid Particle collisions with the Shepherd and the walls of the capsule, that is for "smooth" trajectories which correspond to the standard initial conditions, trajectories with $|y_0| \leq 0.2$ m may be used for orbital altitudes $H_{\rm orb} \leq 1500$ km, while for $H_{\rm orb} = 3000$ km and $x_0 \geq 3$ m, trajectories with $|y_0| = 25$ cm may also be used.

The use of cycloidal trajectories, which appear when the absolute values of the Particle's initial velocity exceed its standard value, make it possible to avoid this limitation.

2.3 Trajectory sensitivity with respect to Newtonian gravitational constant

The influence of the Newtonian gravitational constant G on the Particle motion in the case considered may be investigated by considering how the influence of a small perturbation δG of the "standard" value of G changes the Particle trajectories. Such a perturbation is characterized by the displacement of the perturbed trajectory with respect to the unperturbed one, by an amount equal to

$$\delta \boldsymbol{r} = \boldsymbol{r}_\delta(t) - \boldsymbol{r}_0(t),$$

where $\boldsymbol{r}_\delta$ and $\boldsymbol{r}_0$ denote the radial vectors of the Particle for perturbed and unperturbed motion, respectively. For fairly long trajectories, the displacement along the x axis (δx) may be considered instead of the full displacement ($\delta \boldsymbol{r}$), because numerical simulations show that displacement along the y axis is one order of magnitude less than the displacement along the x axis.

U-shaped Particle trajectories were considered for circular Shepherd orbits in the following range of parameters and initial conditions: orbital altitudes of $H_{\rm orb} = 500$ km, 1500 km and 3000 km and initial position changes in the ranges $2\text{ m} \leq x_0 \leq 5$ m, $-20\text{ cm} \leq y_0 \leq -5$ cm. For comparison with the case where $M = 500$ kg, trajectories with $x_0 = 18$ m were also considered. It was found that the perturbation $\delta G/G = 10^{-6}$ leads to displacement of smooth trajectories by 0.634×10^{-6} m to 3.34×10^{-6} m, with minimal displacement achieved for $y_0 = 0.05$ m, $x_0 = 2$ m and $H_{\rm orb} = 3000$ km while maximal displacement is achieved for $y_0 = 0.05$ m, $x_0 = 5$ m and $H_{\rm orb} = 500$ km.

The use of cycloidal trajectories increases the influence of δG on the Particle's motion.

2.4 Trajectory sensitivity with respect to orbital radius uncertainty

Trajectory sensitivity with respect to the uncertainty in the orbital radius is characterized by the displacement δx, which is induced by a small perturbation (or uncertainty) δh of the orbital altitude $H_{\rm orb}$.*

It was found that for $\delta h = 1$ cm, orbital altitude $H_0 = 1500$ km and $|y_0| = 20$ cm, the maximum value of δx increases from 3.222×10^{-8} m at $x_0 = 2$ m to 9.387×10^{-8} m at $x_0 = 5$ m. For $H_0 = 500$ km these values must be multiplied by a factor of about 2 and for $H_0 = 3000$ km by a factor of approximately 0.5.

It was also found that the dependence of δx on δh may, to a good approximation, be considered linear: in particular, for $\delta h = 1$ m, $H_0 = 1500$ km, $x_0 = 5$ m and $|y_0| = 20$ cm, $\delta x = 9.387 \times 10^{-6}$ m as expected.

*As above, we consider the displacement δx instead of δr because δx provides the main contribution to δr, while δy is much smaller.

The use of cycloidal trajectories reduces the dependence of the trajectories on the orbital altitude. For example, for $H_0 = 1500$ km, $x_0 = 5$ m and $|y_0| = 20$ cm, the uncertainty $\delta h = 1$ cm leads to $\delta x = 1.455 \times 10^{-8}$ m.

It is of note that the influence of the orbital altitude on the Particle's trajectory is greater for the reduced Shepherd mass ($M = 200$ kg) than for the case $M = 500$ kg. For example, for the case where $M = 500$ kg, $H_0 = 1500$ km, $\delta h = 1$ m, $x_0 = 5$ m and $|y_0| = 20$ cm, the displacement of the trajectory becomes $\delta x = 4.6593 \times 10^{-8}$ m.

These estimates yield restrictions on the precision of the Particle trajectory measurements.

2.5 Trajectory sensitivity with respect to Shepherd quadrupole moment uncertainty

The maximal influence of the Shepherd quadrupole moment J_2 on the Particle motion is realized when the axis of the Shepherd is orthogonal to its orbital plane. The influence of δJ_2 on the accuracy of G measurement may be estimated as follows. Let some value of δJ_2 produce the trajectory displacement $|\delta \boldsymbol{r}| \leq \delta l_j$ while the variation δG_0 of G with the same initial conditions gives the trajectory displacement $|\delta \boldsymbol{r}| \leq \delta l_G$. Then, keeping in mind the linear dependence of the trajectory displacements on δJ_2 and δG, the uncertainty in G resulting from the uncertainty δJ_2 may be estimated as

$$\frac{\delta G}{G} \leq \frac{\delta l_j}{\delta l_G} \frac{\delta G_0}{G}.$$

Using this inequality and the results of trajectory simulations, we obtain the estimates given in Table 1 for U-shaped Particle trajectories in circular orbits with $H_{\rm orb} = 1500$ km.

Table 1. Estimates of $\delta G/G$ for $\delta J_2 = 10^{-4}$, when the symmetry axis of the Shepherd is orthogonal to ($\chi = \pi/2$) its orbital plane.

	$10^6 \times \delta G/G$			
y_0/cm	x_0			
	2 m	3 m	4 m	5 m
–5	1.568	5.13	2.41	0.138
–10	3.181	1.41	0.876	0.649
–15	0.857	6.08	5.057	4.486
–20	60.28	44.31	31.91	28.04

One can conclude that uncertainties $\delta J_2 \lesssim 10^{-5}$ do not contribute substantial uncertainty to the measurement of G for most of the trajectories. Only trajectories with $|y_0| = 0.2$ m require $\delta J_2 \lesssim 10^{-6}$ because of the growth in the sinusoidal component for these trajectories.

3. Simulations of experimental procedures

This section describes the results of numerical simulations of the whole measurement procedure aimed at obtaining the sought-after gravitational interaction parameters. These simulations assumed a Shepherd mass of $M = 500$ kg, a circular orbit with $H_{\rm orb} = 1500$ km with a spherical gravitational potential for the Earth, and a Particle mass of 100 g. Where relevant, it is assumed that both the Shepherd and the Particle are made from tungsten. Identical compositions for both are assumed for simplicity as this work is performed for estimation purposes only.

3.1 Simulations of an experiment for measuring G

The constant G is determined from the best-fitting condition between the "theoretical" Particle trajectories ($\boldsymbol{r}_{\rm th}(t_i) = \boldsymbol{r}_{i\_{\rm th}}$), calculated by (2) and (3) for $J_2 = 0$ and the "empirical" ($\boldsymbol{r}_i$) Particle trajectories near the Shepherd. The fitting quality is evaluated by minimizing a function that characterizes a "distance" between the trajectories. We have considered the following functionals for such "distances":

$$S = \sum_{i=1}^{N} \left[(x_i - x_{i\_{\rm th}})^2 + (y_i - y_{i\_{\rm th}})^2 \right], \qquad (5)$$

$$S_x = \sum_{i=1}^{N} (x_i - x_{i\_{\rm th}})^2, \quad S_y = \sum_{i=1}^{N} (y_i - y_{i\_{\rm th}})^2. \qquad (6)$$

The theoretical trajectory depends on the gravitational constant G, on the initial coordinates (x_0, y_0) and on the initial velocities (v_{x0}, v_{y0}). To estimate G, one chooses the value for which a "distance" functional in the space of the five variables $(G, x_0, y_0, v_{x0}, v_{y0})$ reaches its minimum.

We carried out a numerical simulation of the SEE experiment and estimated δG for a given coordinate measurement error ($\sigma = 1 \times 10^{-6}$ m). As "empirical" trajectories, we took computed trajectories with specified values of the above five variables, where Gaussian noise was introduced using a random number generator. Independent "empirical" trajectories were created by non-intersecting random number sequences. The functional was minimized using the gradient descent and consecutive descent methods. The starting value of the "vertical" (along the Earth's radius) coordinate, y_0, was taken to be 0.25 m, while the horizontal one, x_0, varied between 2 m and 18 m. Figure 1 shows the dependence of the uncertainties $\delta G/G$ as a function of initial distance between the bodies; $\delta G/G \equiv R_{\rm grad}$ was obtained by the gradient descent method, and $\delta G/G \equiv R_{\rm s}$ by the consecutive descent method. All the uncertainties are expressed as confidence intervals corresponding to a confidence of 0.95. The mean values of these uncertainties are as follows:

$$R_{\rm grad} = 4.69 \times 10^{-8}, \qquad R_{\rm s} = 5.24 \times 10^{-8}.$$

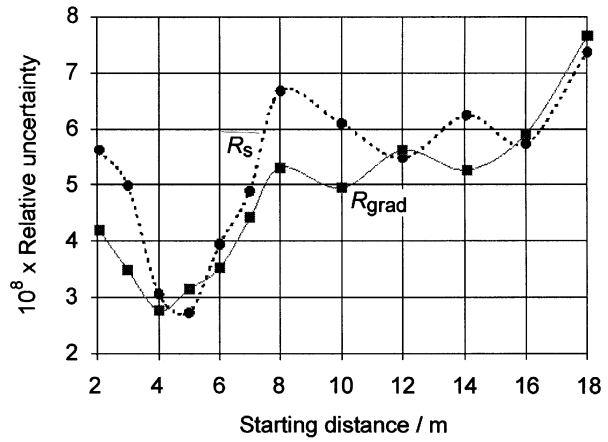

Figure 1. Relative uncertainties $\delta G/G$ estimated by the gradient descent ($R_{\rm grad}$) and consecutive descent ($R_{\rm s}$) methods.

Thus the uncertainties estimated using the gradient and consecutive descent methods are close to each other and about an order of magnitude smaller than that estimated from one-trajectory data. It was found that the simulation results depend strongly on the random number generator, so that ordinary generators are not perfect: the generated random number sets do not have a Gaussian distribution.

The use of a truncated functional such as (6) has shown that a functional incorporating the more informative "horizontal" coordinate x leads to estimates close to those obtained from the total functional, whereas the use of y alone substantially decreases the sensitivity. Therefore in practice, to determine G, it is sufficient to measure only one of the two coordinates, viz. x.

As the "empirical" trajectory is built on the basis of a computed one, with a known value of the gravitational constant G_0, it appears possible to estimate a possible systematic error inherent in the data-processing method. In most cases the latter has turned out to be much smaller than the random uncertainty. This result demonstrates the correctness of the methods used.

As is evident from the results, the best accuracy is achieved at values of x_0 of about 4 m to 5 m (approximately the capsule size).

3.2 Simulation of measurement procedures for estimation of G using velocity data

When the Particle velocity can be precisely measured, the gravitational constant can be estimated from the velocity data alone. A computer program was created for simulating an experiment determining the gravitational constant G by velocity data. These simulations assumed a Shepherd mass of 500 kg, a circular orbit with $H_{\rm orb} = 1500$ km (spherical Earth's potential), a Particle mass of 100 g, and an uncertainty in the velocity of $\delta v_x = 1 \times 10^{-8}$ m/s. The constant G is estimated from the best-fitting condition between the theoretical Particle velocity ($\boldsymbol{v}_{\rm th}(t_i) \equiv \boldsymbol{v}_{i-{\rm th}}$) and the empirical one. The fitting quality is evaluated by minimizing a functional characterizing a distance between velocity trajectories. We used the following:

$$V = \sum_{i=1}^{N} \Big[(v_{xi} - v_{xi\_{\rm th}})^2 + (v_{yi} - v_{yi\_{\rm th}})^2 \Big].$$

The theoretical velocity depends on the gravitational constant G, on the initial coordinates (x_0, y_0), and the initial velocities (v_{x0}, v_{y0}). To estimate G, one chooses the value for which the velocity distance functional V reaches its minimum in the space of the five variables $(G, x_0, y_0, v_{x0}, v_{y0})$.

As empirical trajectories, we took computed trajectories with specified values of the above five variables, where Gaussian noise was introduced using a random number generator. Independent empirical trajectories were created by non-intersecting random number sequences. The functional V was minimized using the gradient descent method. The starting value of the y_0 coordinate was taken to be 0.25 m, while the horizontal one, x_0, varied between 2 m and 6 m. The value of G was estimated from eleven trajectories. Appropriate uncertainties were estimated at confidence intervals corresponding to a confidence of 0.95 and expressed relative to G; values of $\delta G/G\Big|_{VR}$ are plotted in Figure 2. The relative uncertainty $\delta G/G\Big|_{CR}$ obtained using the coordinate functional for a coordinate measurement uncertainty of $\sigma = 1 \times 10^{-6}$ m is also

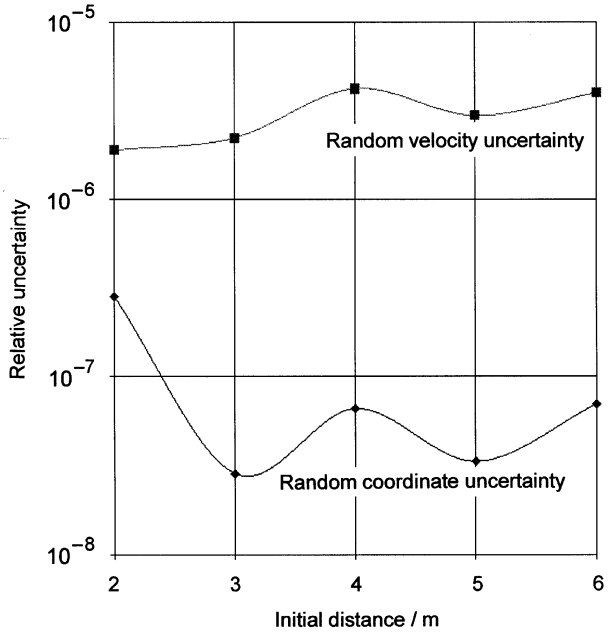

Figure 2. Random "velocity" and "coordinate" uncertainties.

shown in the same figure. Computer-based simulation also allows systematic errors to be estimated. We see that for a given set of measurement uncertainties the accuracy of estimation of G is better using the coordinate functional.

3.3 Equations of motion with Yukawa terms

We present the Particle equations of motion in the relevant approximation, including the contributions from hypothetical Yukawa forces, taking into account the finite size of the Yukawa field sources.

Let the interaction potential for two elementary masses m_1 and m_2 be described by the potential

$$\mathrm{d}V_{\mathrm{Yu}} = \frac{G\,\mathrm{d}m_1\mathrm{d}m_2}{r}\alpha\,\mathrm{e}^{-r/\lambda}, \tag{7}$$

where r is the separation of the masses, and α and λ are the strength and range of the Yukawa forces. Then for two massive bodies with radii R_1 and R_2, after integration over their volumes we obtain [20]

$$V_{\mathrm{Yu}} = \frac{G\,m_1 m_2 \beta_1 \beta_2}{r}\alpha\,\mathrm{e}^{-r/\lambda}, \tag{8}$$

where

$$\beta_i = 3\left(\frac{\lambda}{R_i}\right)^3\left[\frac{R_i}{\lambda}\cosh\frac{R_i}{\lambda} - \sinh\frac{R_i}{\lambda}\right]. \tag{9}$$

When $R_i/\lambda \ll 1$, we have $\beta_i \approx 1$. This may be the case when we consider the interaction between the Shepherd and the Particle at a distance of the order of a few metres. The radii of the Shepherd and the Particle are small: $R_1 \approx 18$ cm for the Shepherd and $R_2 \approx 1.1$ cm for the Particle. If the range λ is of the order of the Earth's radius, $\lambda \approx R_\oplus$, we have $\beta_\oplus = 1.10$ and $\beta_{1,2} = 1$ where the indices 1 and 2 designate Shepherd and Particle, respectively.

Equations of motion are obtained under the following assumptions. There are two Yukawa interactions with the parameters λ_0 and α_0, referring to the Earth-Shepherd and Earth-Particle interactions which are the same (due to the assumed identical compositions of the Shepherd and the Particle), while λ and α determine the Shepherd-Particle interaction. The equations of motion in the frame of reference of the Shepherd, with the same notations for x, y and s as used previously, are

$$\begin{aligned}
&\ddot{x} + 2\omega^2\dot{y} + G(m_1+m_2)\frac{x}{s^3} - 3\omega^2\frac{xy}{s} + \\
&\quad G(m_1+m_2)\frac{x}{s^3}\alpha\left(1+\frac{s}{\lambda}\right)\mathrm{e}^{-s/\lambda} = 0; \\
&\ddot{y} - 2\omega\dot{x} - 3\omega^2 y + \\
&\quad G(m_1+m_2)\frac{y}{s^3} + \frac{3\omega^2}{r_{01}}\left(y^2 - \frac{x^2}{2}\right) + \\
&\quad G(m_1+m_2)\frac{y}{s^3}\alpha\left(1+\frac{s}{\lambda}\right)\mathrm{e}^{-s/\lambda} - \\
&\quad \omega^2\beta_0\alpha_0\,\mathrm{e}^{-r_{01}/\lambda_0}y = 0,
\end{aligned} \tag{10}$$

where ω is the orbital frequency:

$$\omega^2 = \frac{GM_\oplus}{r_{01}^3}\left[1 + \beta_0\alpha_0\left(1+\frac{r_{01}}{\lambda_0}\right)\mathrm{e}^{-r_{01}/\lambda_0}\right]. \tag{11}$$

We have neglected the terms quadratic in s/r_{01} times α or α_0 due to their manifestly small contributions.

If we set $\alpha_0 = 0$ in (10), we obtain the equations used to describe only the Shepherd-Particle Yukawa interaction. Note that the Yukawa terms are roughly proportional to the gradients of the corresponding Newtonian accelerations, i.e. Gm_1/s^3 for the Shepherd-Particle interaction and $GM_\oplus/r_{01}^3 \approx \omega^2$ for (say) the Earth-Shepherd interaction. In our case these quantities are estimated as

$$\begin{aligned}
&Gm_1/s^3 \approx 2.7\times10^{-10}\ \mathrm{s}^{-2} \qquad \text{for}\ \ s = 5\ \mathrm{m}, \\
&\text{and}\quad \omega^2 \approx 8.16\times10^{-7}\ \mathrm{s}^{-2}.
\end{aligned} \tag{12}$$

Thus, given the same strength parameter, the Earth's Yukawa force is three orders of magnitude greater than that between the Shepherd and the Particle. Therefore, some significant progress might be expected in an ISL test for λ of the order of the Earth's radius.

Equations (10) were used to simulate the measurement procedures.

3.4 Sensitivity to Yukawa forces with $\lambda \approx 1$ m

In an experiment to detect the Yukawa interaction between the Shepherd and the Particle using the potential (8) with $\beta_{1,2} = 1$, two theoretical trajectories are computed: the first ignoring the Yukawa forces $(x_0(t_i),\ y_0(t_i))$ and the second taking them into account $(x_\alpha(t_i),\ y_\alpha(t_i))$. These two computed curves are compared with the empirical trajectory using the function S_k $(k = 0, \alpha)$ according to (5) which may be considered as a dispersion characterizing a scatter of the "empirical" coordinates with respect to the fitting trajectory. This is true when the theoretical model is adequate for the real situation. In the case $k = \alpha$ the functional $S_k = S_\alpha$ has a χ^2 distribution with $n_2 = 2N - 1$ degrees of freedom. With $k = 0$ the parameter α is absent, therefore S_0 is distributed according to the χ^2 law with $N_1 = 2N$ degrees of freedom. Then their ratio $S_0/S_\alpha = F_{n_2,n_1}$ will be distributed according to the Fischer law [21] with n_2 and n_1 degrees of freedom. If an experiment shows that, at a given significance level q, the relation (see [11])

$$S_0/S_\alpha \geq F_{n_1,n_2,q} \tag{13}$$

is valid, one should conclude that the Yukawa force has been detected. Equality in (13) represents the minimum detectable force for the given significance level q. We have assumed $q = 0.95$. Figure 3 presents the results of a sensitivity computation for different values of the space parameter λ (curve 1). A maximum sensitivity of $\alpha = 2.1\times10^{-7}$ is observed for $\lambda = 1.25$ m. This value is three to four orders of magnitude better than the sensitivity of terrestrial experiments in the same range.

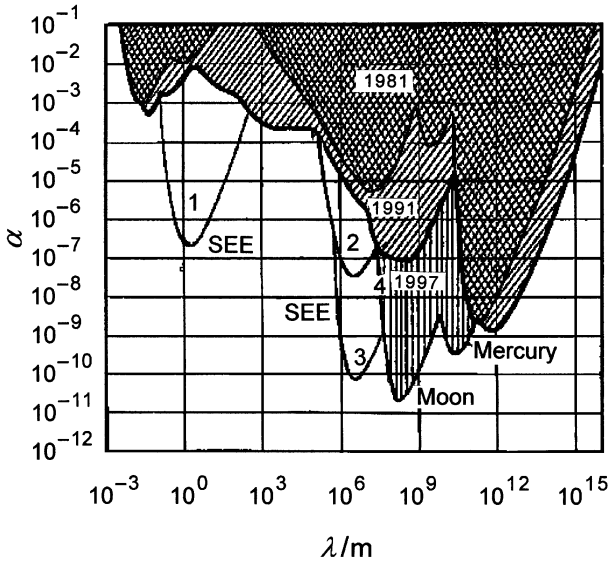

Figure 3. The sensitivity of the SEE method to Yukawa forces with the range parameter λ_0 of the order metres (1) of the Earth's radius $R_\oplus$ using (2) trajectory measurements and (3) orbital precession. The limitations on Yukawa forces parameters from [11] (4).

3.5 Sensitivity to Yukawa forces with $\lambda \approx R_\oplus$

To estimate the parameter α_0 in (10), computer simulations were carried out using the method described above for α, based on the Fischer criterion for the significance level 0.95. The range parameter λ_0 varied from $(1/32)R_\oplus$ to $32R_\oplus$. Two trajectories were calculated, with initial Shepherd-Particle separations x_0 of 2 m and 5 m. In both cases the impact parameter y_0 was chosen to be 0.25 m. We used (10) with $\alpha = 0$, i.e. excluding the non-Newtonian interaction between Shepherd and Particle. As is evident from (10), the Particle trajectory depends on the ratio r_{01}/λ_0 in the product $(r_{01}/\lambda_0)\,\mathrm{e}^{-r_{01}/\lambda_0}$. This quantity reaches its maximum at $\lambda_0 = r_{01}/2$. Our calculations have confirmed that a maximum sensitivity of the SEE method (3.4×10^{-8} for $x_0 = 5$ m) is indeed observed at this value of λ_0. This is about an order of magnitude better than the estimates obtained by other methods. It is hoped that this estimate can be further improved by about an order of magnitude by optimization of the orbital parameters. However, one factor that can, to a certain extent, spoil these results, is the uncertainty in the parameter ω which, in this calculation, was assumed to be known precisely.

The simulation results are shown in Figure 3 (curve 2) for a trajectory with an initial Shepherd-Particle separation of 5 m; See the next section for further discussion of this figure.

3.6 Precession of Shepherd orbit and a test of inverse-square law at distances of the order of R_E

We have shown previously that the SEE experiment allows the inverse-square law to be tested at distances of the order of 1 m ($\alpha_{\min} \approx 2 \times 10^{-7}$) and of the order of half the orbital radius ($\alpha_{\min} \approx 3.4 \times 10^{-8}$) [22]. The law can also be tested using spacecraft precession data. It is known that in two-body problems an orbit is closed for only two potentials: (i) the Newtonian potential, $U \sim 1/r$; and (ii) $U \sim r^2$. In other cases the orbit is not closed and a pericentre precession is observed. In particular, any deviation from the Newtonian law entails a precession of the orbit due to the Yukawa interaction. For

$$U' = \frac{Gm_1m_2}{r}\alpha\,\mathrm{e}^{-r/\lambda}, \tag{14}$$

the Shepherd orbit exhibits a precession. In general, the precession magnitude due to a small perturbation, described by a potential δU, is given by (see [1])

$$\delta\varphi = \frac{\partial}{\partial M}\left(\frac{2m'}{M}\int_0^\pi r^2\delta U\,\mathrm{d}\varphi\right). \tag{15}$$

The integration is carried out over the non-perturbed trajectory. Here m is the mass of the Shepherd, m' is the mass of a central body (the Earth), $M = mr^2\dot{\varphi}$ is an integral of motion (the angular momentum), and $\delta U = \alpha(Gmm')\,\mathrm{e}^{-r/\lambda}$. The non-perturbed trajectory is described by the expressions

$$\begin{aligned} &r = \frac{p}{1+e\cos\varphi}, \qquad p = \frac{M^2}{m(Gmm')}, \\ &e^2 = 1 + \frac{2EM^2}{m(Gmm')^2}, \qquad p = a(1-e^2). \end{aligned} \tag{16}$$

After a standard algebraic computation we obtain

$$\begin{aligned} \delta\varphi = \alpha\frac{2}{e}\int_0^\pi \frac{\exp(-r/\lambda)}{(1+e\cos\varphi)^2}\times \\ \left\{\frac{1}{\lambda}\left[2e+(1+e^2)\cos\varphi\right]-(e+\cos\varphi)\right\}\mathrm{d}\varphi, \end{aligned} \tag{17}$$

where

$$\frac{r}{\lambda} = \frac{a}{\lambda}\,\frac{1-e^2}{1+e\cos\varphi}. \tag{18}$$

Using (8) and data with the error $\delta\varphi$ for the SEE Satellite, we calculated the curves $\alpha(\lambda)$, which determine the border on the α-λ plane between two domains: where the Yukawa interaction (a new long-range force) is forbidden by experiment, and where it is not. The sensitivities to Yukawa interactions are shown in Figure 3 as curve 4 (see [10]) for the parameter λ in the range 1×10^6 m to 1×10^{13} m. Curve 3 was calculated for the SEE satellite with an eccentricity $e = 0.01$ and the precession error $\delta\varphi = 0.1''/y$.

One can conclude that the ISL may be tested with a sensitivity of $\alpha \approx 6.3 \times 10^{-11}$ for $\lambda \approx 3.9 \times 10^6$ m (half the orbital radius).

4. A possible effect of the Earth's radiation belt

Charged particles, penetrating into the SEE capsule from space and captured by the test bodies, create electrostatic forces that could substantially distort the experimental results. The sources of such particles include (i) cosmic-ray showers, (ii) solar flares, and (iii) the Earth's radiation belts (Van Allen belts). The effect of cosmic-ray showers was estimated in [1] and shown to be negligible. Solar flares are fairly rare events and, although they create very significant charged particle fluxes, sometimes even exceeding those in the most dense regions of the radiation belts, it can be assumed that the SEE measurements (except those of $\dot{G}$) are stopped for the period of an intense flare. In contrast, the effect of the Van Allen belts is permanent as long as the satellite orbit passes, at least partially, inside them.

We show here that the charging is unacceptably high at otherwise favourable satellite orbits, so that some kind of charge removal technique is necessary, but this problem can be addressed reasonably easily using currently available technology.

The range of the most favourable SEE orbital altitudes, roughly 1400 km to 3300 km [1], coincides with the inner region of the so-called inner radiation belt [23-26], situated presumably near the plane of the magnetic equator. This region is characterized by a considerable flux of high-energy protons and electrons. For an SEE satellite at altitudes near 1500 km the duration of the charging periods is about 12 minutes. Maximum charging rates occur over the central Atlantic. It should be noted that the South Atlantic Anomaly (SAA) – a region of intense Van Allen activity which results from the low altitude of the Earth's magnetic field lines over the South Atlantic Ocean — cannot cause additional problems for the SEE experiments. The reason is that the SAA mostly contains low-energy protons which cannot penetrate into the SEE capsule.

Electrons are known to be stopped by even a thin metallic shell, so only protons are able to induce charges on the test bodies. Proton-induced charges on the test bodies can create considerable forces. The inner radiation belt contains protons with energies of 20 MeV to 800 MeV, and their maximum fluxes at an altitude of 3000 km over the equator are as great as about $3 \times 10^6\ \mathrm{cm^{-2}\ s^{-1}}$ for energies $E \gtrsim 10^6$ eV and about $2 \times 10^4\ \mathrm{cm^{-2}\ s^{-1}}$ for $E \gtrsim 10^7$ eV. At 1500 km altitude the fluxes are a few times smaller; they gradually decrease with growing latitude φ and vanish at $\varphi \approx 40°$.

It is important that estimates of any resulting effects take into account that (i) the capsule walls have a considerable thickness and stop the low-energy part of the proton flux and (ii) among the protons that penetrate the capsule and hit the Particle, the most energetic ones, whose path in the Particle material is longer than the Particle diameter, fly through it and hit the capsule wall again. As for the Shepherd, its size is large enough to stop the overwhelming majority of protons that hit it.

In what follows, we assume a Shepherd radius of 20 cm and a Particle radius of 2 cm and estimate the captured charges for some satellite orbits in a capsule whose walls of aluminium are 2 cm, 4 cm, 6 cm and 8 cm thick. The SEE satellite must actually involve several coaxial cylinders for thermal-radiation control, and the combined thickness of their walls must amount to several centimetres. We assume, in addition, that the Particle also consists of aluminium and stops all protons whose path is shorter than 4 cm (thus overestimating the charge by a small amount as most of the protons will cover a shorter path through the Particle material). A 100 g Particle of aluminium will have a radius of about 2.07 cm.

It is advisable to first determine which charges (and fluxes that create them) might be neglected.

4.1 Admissible charges

Let us estimate the Coulomb interaction both between Shepherd and Particle and between each test body and its image in the capsule walls. To estimate the spurious effects on the Particle trajectory, it is reasonable to calculate its possible displacements due to the Coulomb forces from the growing number of captured charged particles. We assume that the test bodies are discharged by grounding to the capsule before launching the Particle in each given experiment.

Criterion. We call the induced charges, or the fields they create, *admissible* if they cause a displacement of the Particle with respect to the Shepherd smaller than a prescribed coordinate measurement error δl (we take here $\delta l = 10^{-6}$ m) for a prescribed measurement time (we take $t \geq 10^4$ s).

The Coulomb acceleration $a_Q(t) = q_M q_m/(4\pi\varepsilon r^2 m)$ (where ε is the absolute permittivity of the medium) depends on the Shepherd-Particle separation r and on the form of the function $J(t)$, which in turn depends on the satellite orbital motion.

The charge-induced Particle displacement is approximately

$$\Delta l = \int \mathrm{d}t \left[\int \mathrm{d}t\, a_Q(t) \right] \tag{19}$$

as the acceleration is almost unidirectional. If, for estimation purposes, we suppose that the flux $J(t, x)$ is time-independent, then the resulting displacement is

$$\Delta l \approx \frac{1}{30}\ \frac{\bar{e}^2 S_M S_m J_0^2 t^4}{r^2 m}, \tag{20}$$

where $S_M \approx 1256\ \mathrm{cm^2}$ is the Shepherd cross-section, $S_m \approx 12.56\ \mathrm{cm^2}$ is the Particle cross-section, m is the Particle mass, r is an average Shepherd-Particle separation, and $\bar{e}$ is the electron charge.

The strong time dependence is explained by the rapid growth of the Coulomb force due to increasing charges. Numerically, with the above values of S_M and S_m, taking $m = 100$ g and $r = 1$ m (the latter leads to an overestimated force as the Particle spends most of the time at greater distances), we find:

$$J_0^2 t^4 \lesssim 0.83 \times 10^{18} \text{ s}^2 \text{ cm}^{-4}. \quad (21)$$

For $t = 10^4$ s an admissible flux is thus less than $9 \text{ cm}^{-2} \text{ s}^{-1}$.

Another undesired effect is that the Particle, being charged by the belt protons, will interact with the capsule walls. This is well approximated as an interaction with the Particle's mirror image in the wall, while the latter may be roughly imagined as a conducting plane. Then, assuming that the Particle is on average about 25 cm from the capsule wall and using the same kind of reasoning as above, instead of (21) we obtain

$$J_0^2 t^4 \lesssim 2.07 \times 10^{19} \text{ s}^2 \text{ cm}^{-4}, \quad (22)$$

and an admissible proton flux less than $45 \text{ cm}^{-2} \text{ s}^{-1}$ for $t = 10^4$ s.

Other estimates are also of interest: if the charge can be kept smaller than a certain value, then what is the upper limit for it to create only negligible displacements? Suppose that there are constant charges on both the Shepherd ($q = q_M$) and the Particle ($q = q_m$, $m = 100$ g), then they are admissible according to the above criterion as long as

$$q_M q_m < 2.2 \times 10^{-25} \text{ C}^2, \quad (23)$$

$$q_m^2 < 5.6 \times 10^{-26} \text{ C}^2. \quad (24)$$

These inequalities follow, respectively, from considering the Shepherd-Particle interaction and the interaction between the Particle (located at 25 cm from the wall) and its image. Thus the maximum admissible Particle charge is about $1.5 \times 10^6 \bar{e}$. Assuming this value, it follows from (23) that the maximum Shepherd charge is about $5.5 \times 10^6 \bar{e}$. With these charge values the electric potentials on the test-body surfaces are

$$U_M \approx 45 \text{ mV};$$

$$U_m \approx 105 \text{ mV}. \quad (25)$$

If the requirements (23), (24) are satisfied (e.g. the potentials are kept smaller than the values (25)), the electrostatic effect on the Particle trajectory may be neglected.

The Shepherd's interaction with the respective image charge induced at the nearest location to it in the SEE experimental chamber does not lead to appreciable Particle displacements. A very demanding requirement on the Shepherd charge emerges, however, if the SEE satellite is used for $\dot{G}$ determination (a detailed discussion of which is postponed to future papers). In this case,

$$U_M \lesssim 1 \text{ mV}. \quad (26)$$

Evidently, in this case the Shepherd-Particle interaction per se is not the determining factor with respect to charge limits on the test bodies.

4.2 Captured charges in certain orbits

The charges captured by Shepherd and Particle on board a satellite in various circular orbits for a single revolution around the Earth (a period of about 2 hours) were estimated in [22]. (Actual measurement times may exceed this period, but not by much.) These estimates were obtained with the aid of SEE2 and SEREIS software developed at the Nuclear Physics Institute of Moscow State University [27].

The results obtained lead to a number of conclusions of importance to the SEE experiments (details in [22]).

First, the models show zero proton fluxes in equatorial orbits of 500 km to 800 km altitude but indicate considerable fluxes at the same altitudes when crossing the SAA. It turns out, however, that the SAA is overwhelmingly a low-energy phenomenon and leaves the fluxes virtually unaffected on the relevant energy scale, beginning at approximately 65 MeV. Moreover, there is a very small proton flux due to the SAA even at energies above 10 MeV; hence with 1 mm layer of shielding the SAA influence is negligible. Behind a thicker layer of shielding there are no secondary particles due to SAA protons.

Second, at an altitude of 1500 km the fluxes depend substantially on the orbit orientation but remain on the same scale of a few million protons per cm^2 at energies over 65 MeV.

Third, at an altitude of 3000 km both the total flux and its high-energy component in particular are a few times greater than at 1500 km.

Fourth, and most important: for all orbits in the desirable range of altitudes the charges are quite large compared with their admissible values and they remain large even behind relatively thick walls. It is thus important to have a means of detecting and removing these charges during measurements. Moreover, as seen from the peak values in Table 2 and time scans of Van Allen charging in orbits of interest (1500c is one of the most favourable, 1500b is less favourable; the data were again obtained using the above-mentioned software), at a charging peak, when crossing the magnetic equator, the time required for the charges on the test bodies to reach their maximum allowable values, as listed above, is a matter of seconds, not minutes. Therefore the charge must be detected and removed as it builds up, on a time scale of seconds.

Table 2. Average flux, peak flux and captured charges per revolution in some satellite orbits

Orbit	Wall thick-ness/cm	Average flux/ $(\mathrm{cm}^{-2}\ \mathrm{s}^{-1})$	Peak flux/ $(\mathrm{cm}^{-2}\ \mathrm{s}^{-1})$	Shepherd charge $q_M/\bar{e}$	Particle charge $q_m/\bar{e}$
	2	1420	12 300	1.5×10^{10}	4.5×10^{7}
1500b	4	1000	8 800	1×10^{10}	2.6×10^{7}
	6	770	6 800	7.5×10^{9}	1.5×10^{7}
	8	600	5 400	6×10^{9}	1.2×10^{7}
	2	646	5 700	6.5×10^{9}	1.9×10^{7}
1500c	4	464	4 200	4.3×10^{9}	1.1×10^{7}
	6	365	3 300	3.5×10^{9}	7×10^{6}
	8	280	2 700	2.7×10^{9}	5×10^{6}

The detection and measurement of the charge on the test bodies can probably be achieved relatively easily by an array of minute microvoltmeters attached to the inner wall of the experimental chamber.

Several methods for removing positive charge are now being evaluated. A simple and promising method may be to shoot electron beams directly at test bodies. The number of electrons needed is of the order of $10^8/\mathrm{s}$. Although this approach has the inherent drawback that it requires an active system to perform correctly for many years, it is simple in principle and will accomplish the goal.

5. Concluding remarks

The main results of the recent developments described in this paper may be summarized as follows:

1. Numerical simulations of the Particle relative motion in the case of a lighter Shepherd (200 kg), for initial Particle-Shepherd separations between 2 m and 5 m and for $H_{\mathrm{orb}} = 500$ km to 3000 km, have shown that the trajectories are not much more sensitive to changes of G than those previously estimated for a heavier Shepherd (500 kg). In particular, variations $\delta G/G \approx 10^{-6}$ lead to trajectory shifts along the x axis ranging from 0.634×10^{-6} m to 3.34×10^{-6} m.

It has been found that an error of 1 cm in H_{orb} leads to trajectory shifts of 3×10^{-8} m to 10^{-7} m, i.e. about an order of magnitude smaller than the planned coordinate measurement error, 10^{-6} m, and the trajectory shifts due to G variations, of 1 part in 10^6.

The estimated relative uncertainty in G due to Shepherd non-sphericity, characterized by its quadrupole moment $J_2 \approx 10^{-5}$, is close to 10^{-6}; this places rather severe requirements upon the precision of fabrication of the Shepherd. The same quadrupole moment causes even greater $\delta G/G$ if the Particle motion starts at $y_0 > 15$ cm.

2. Computer simulations have shown that the gravitational constant G can be measured up to about 5×10^8. The inverse-square law may be tested with a sensitivity of $\alpha \approx 2\times10^{-7}$ for $\lambda = 1.2$ m and $\alpha \approx 3\times10^{-8}$ for $\lambda \approx 3.4\times10^6$ m (half the Earth's radius). Observation of the precession of the Shepherd orbit makes it possible to test the inverse-square law at $\lambda \approx 3.4\times10^5$ m with a sensitivity of up to 10^{-10}.

3. Estimation of test-body charging due to crossing the Van Allen radiation belts shows that this effect requires special means for charge measuring and removal. These means, however, do not go beyond the currently available technology.

Acknowledgements. This work was supported in part by NASA grant # NAG 8-1442. K.A.B. wishes to thank Nikolai V. Kuznetsov for helpful discussions and for providing access to the SEE2 and SEREIS software. V.N.M. is grateful to CINVESTAV and CONACYT for their hospitality and support during his stay in Mexico.

References

1. Sanders A. J., Deeds W. E., *Phys. Rev.*, 1992, **D46**, 489-504.
2. de Sabbata V., Melnikov V. N., Pronin P. I., *Prog. Theor. Phys.*, 1992, **88**, 623-661.
3. Melnikov V. N., *Int. J. Theor. Phys.*, 1994, **33**(7), 1569.
4. Gillies G. T., *Rep. Prog. Phys.*, 1997, **60**, 151-225.
5. Fitzgerald M. P., Armstrong T. R., Recent Results for g from MSL Torsion Balance, In *The Gravitational Constant: Theory and Experiment 200 Years after Cavendish* (23-24 November 1998), Cavendish-200 Abstracts, London, Institute of Physics, 1998.
6. Schurr J., Nolting F., Kündig W., *Phys. Rev. Lett.*, 1998, **80**, 1142.
7. Meyer H., Value for G Using Simple Pendulum Suspensions, In *The Gravitational Constant: Theory and Experiment 200 Years after Cavendish* (23-24 November 1998), Cavendish-200 Abstracts, London, Institute of Physics, 1998.
8. Karagioz O. V., Izmaylov V. P., Gillies G. T., *Grav. & Cosmol.*, 1998, **4**(3), 239-245.
9. Gundlach J. H., Merkowitz S. M., *Phys. Rev. Lett.*, 2000, **85**, 2869-2872.
10. Fischbach E., Talmage C., *Mod. Phys. Lett.*, 1989, **A4**, 2303-2310; *Nature (London)*, 1992, **356**, 207-215.
11. Fischbach E., Talmage C., In *International Workshop on Gravitation and Astrophysics*, Tokyo, Japan, 17-19 November 1997, 1-9.
12. Roll P. G., Krotkov R., Dicke R. H., *Ann. Phys. (NY)*, 1964, **26**, 442-517.
13. Braginsky V. B., Panov V. I., *Zh. Eksp. Teor. Fiz.*, 1971, **61**, 873-875 [*Sov. Phys.-JETP*, 1972, **34**, 463].
14. Achilli V. et al., *Nuovo Cimento*, 1997, **112B**(5), 775-804.
15. Adelberger E. G., *Class. Quantum Grav.*, 1994, **11**, A9-A21.
16. Fischbach E., Gillies G. T., Krause D. E., Schwan J. G., Talmadge C., *Metrologia*, 1992, **29**(3), 213-260.
17. Franklin A., *The Rise and Fall of the Fifth Force: Discovery, Pursuit, and Justification in Modern Physics*, New York, American Institute of Physics, 1993.
18. Alexeev A. D., Bronnikov K. A., Kolosnitsyn N. I., Konstantinov M. Yu., Melnikov V. N., Radynov A. G., *Izmeritel'naya Tekhnika*, 1993, **8**(6-10), **9**(3-6), **10**(6-9), 1994, **1**(3-5).

19. Alexeev A. D., Bronnikov K. A., Kolosnitsyn N. I., Konstantinov M. Yu., Melnikov V. N., Radynov A. G., *Int. J. Mod. Phys.*, 1994, **D3**(4), 773-793.
20. Zaitsev N. A., Kolosnitsyn N. I., In *Experimental Tests of Gravitation Theory*, Moscow, Moscow University Press, 1989, 38-50 (in Russian).
21. Brandt S., *Statistical and Computational Methods in Data Analysis*, Heidelberg, Heidelberg University Press, 1970.
22. Alexeev A. D., Bronnikov K. A., Kolosnitsyn N. I., Konstantinov M. Yu., Melnikov V. N., Sanders A. J., *Grav. & Cosmol.*, 1999, **5**(1), 67-78.
23. Tverskoy B. A., *Dynamics of the Earth's Radiation Belts*, Moscow, Nauka, 1968 (in Russian).
24. Galperin Yu. I., Gorn L. S., Khazanov B. I., *Radiation Measurements in Space*, Moscow, Atomizdat, 1972 (in Russian).
25. Williams D. J., ESSA Technical Report ERL 180-SDL16, 1970; Dessler A. J., O'Brien B. J., In *Satellite Environment Handbook*, 2nd ed. (Edited by F. S. Johnson), Stanford, Calif., Stanford University Press, 1965, 53-92.
26. Hess W. N., *The Radiation Belt and Magnetosphere*, Waltham, Mass., Ginn Blaisdell, 1968.
27. Bashkirov V. F., Kuznetsov N. V., Nymmik R. A., Information system for evaluation of space radiation environment and radiation effects on spacecraft, "Space Radiation Environment Modelling: New Phenomena and Approaches" workshop , 7-9 October 1997, Program and Abstracts, 4.8.

Received on 9 May 2000 and in revised form on 24 February 2001.